



OPEN

Enhancing accuracy and convenience of golf swing tracking with a wrist-worn single inertial sensor

Myeongsub Kim & Sukyung Park

In this study, we address two technical challenges to enhance golf swing trajectory accuracy using a wrist-worn inertial sensor: orientation estimation and drift error mitigation. We extrapolated consistent sensor orientation from specific address-phase signal segments and trained the estimation with a convolutional neural network. We then mitigated drift error by applying a constraint on wrist speed at the address, backswing top, and finish, and ensuring that the wrist's finish displacement aligns with a virtual circle on the 3D swing plane. To verify the proposed methods, we gathered data from twenty male right-handed golfers, including professionals and amateurs, using a driver and a 7-iron. The orientation estimation error was about 60% of the baseline, comparable to studies requiring additional sensor information or calibration poses. The drift error was halved and the single-inertial-sensor tracking performance across all swing phases was about 17 cm, on par with multimodal approaches. This study introduces a novel signal processing method for tracking rapid, wide-ranging motions, such as a golf swing, while maintaining user convenience. Our results could impact the burgeoning field of daily motion monitoring for health care, especially with the increasing prevalence of wearable devices like smartwatches.

Golf is a sport that is greatly influenced by the swing mechanics of multi-body segments and the club. Players and coaching staffs have a high demand for golf swing monitoring to improve golf performance and prevent injuries¹. In recent years, with the development of micro sensors and smart devices, there has been an exponential surge in the demand for sophisticated swing monitoring technologies. This has led to a rapid increase in the development of golf monitoring products and golf biomechanics researches^{1–11}. Advancements in image processing and deep learning technologies have recently led to numerous studies on methods of golf swing monitoring, such as joint trajectories and swing postures, and club trajectories, etc. Jia et al. estimated the wrist trajectory during a golf swing to be around 17 cm and 10 cm error levels, respectively, through the use of a depth camera alone and in combination with inertial sensors¹¹. Park et al. applied a machine learning algorithm, random forest, to depth camera images to estimate the positions of key joints during a golf swing, with an error level of approximately 3 cm¹². Ko et al. estimated the rotation angles of multiple body segments from images of a single RGB camera, with an error level of 3–8° per axis¹³. Nam et al. estimated the club trajectory to an error level of 13.2 cm by integrating information from an inertial sensor attached to the club and stereo camera images¹⁴. Although the development of artificial intelligence technologies has led to an increase in research on image-based golf tracking, the use of sensors such as cameras to obtain image data limits the convenience of monitoring golf swings in the field. To ensure the convenience of golf swing monitoring, wearable devices based on inertial sensors are being utilized in the field of golf swing monitoring. Kim et al. analyzed the accelerations during golf swing movements using two inertial sensors attached to the left and right wrists, and calculated the average swing trajectory¹⁵. King et al. calculated the putter head trajectory using an inertial sensor located at the end of the club during robotic putting¹⁶. Jensen et al. estimated the time spent in each phase of putting using machine learning algorithm applied to the inertial sensor data acquired from the putter head¹⁷. Cheon et al. estimated the club head trajectory using a single inertial sensor attached to the grip part of the club¹⁸. Jia et al. examined technical issues during an inertial sensor-based golf swing, reporting that the accuracy of trajectory estimation is decreased due to noise from the inertial sensor and that a 30–60 cm level of error occurs depending on the attachment location of the inertial sensor, given the large variability and fast action of golf swings¹¹. Most of the previous studies have the

Department of Mechanical Engineering, Korea Advanced Institute of Science and Technology, Daejeon 34141, South Korea. email: sukyungp@kaist.ac.kr

location of the inertial sensor attachment on the club rather than the body and the information of the swing being monitored is mainly the acceleration or angular speed measured directly from the inertial measurement unit (IMU). Although trajectories of body segments during swing are more intuitive tracking information for golfers than velocity or acceleration, there are not many studies or commercial products that provide quantitative swing trajectory information, due to the limited accuracy in trajectory estimation.

In the pursuit of enhancing the accuracy of swing trajectory estimation using inertial sensors, particularly when the number and placement of sensors are constrained for user convenience, the following technical issues need to be addressed to improve accuracy: First, from the swing data measured by the inertial sensor, we need to robustly identify major sequences of a golf swing, such as the address (ADD), backswing top (BST), impact (IMP), and finish (FIN), despite differences in swing style according to skill level and type of club. Previous studies have attempted to perform segmentation using traditional signal processing methods, heuristic methods, and machine learning algorithms. Jensen et al. applied machine learning techniques to the inertial sensor data attached to the putter head to calculate the major phases of putting¹⁷, while Kooyma et al. used a heuristic method based on the zero-crossing moments of angular velocity¹⁹. Heuristic methods utilizing IMU signal threshold values have been applied to the segmentation of inertial sensor data attached to the club²⁰ and the grip²⁰. Other studies have explored segmentation of golf swing phases using IMUs attached to the body rather than the club. For instance, Kim et al. compared the accuracy of heuristic method, Convolutional Neural Network (CNN), and Bidirectional Long Short-Term Memory (BLSTM) in segmenting inertial sensor data from various body parts such as the wrist, waist, and head. They reported that machine learning-based segmentation demonstrated high accuracy²¹.

The second technical issue that needs to be addressed to improve accuracy is calibrating the sensor orientation. To calculate the swing trajectory from an inertial sensor attached to the body or club, it is necessary to know the sensor orientation that transforms the relative coordinate system at the attachment point to the absolute coordinate system of the ground. For this, the sensor orientation at the start of the motion, mostly the ADD, is first estimated, and then, using this value as an initial condition, the rotation of the sensor coordinate system over the entire range of the motion is calculated by integrating the angular velocity signal measured from the inertial sensor²². During the integration process, errors caused by bias and scale factors of the inertial sensor signals accumulate over time²³, and there have been reports indicating that fast rotational motions with a large angular velocity result in more significant orientation errors²⁴. The typical method of estimating the initial posture's sensor orientation involves temporarily placing the inertial sensor on a known coordinate system like the ground or a table, where only gravitational acceleration is present, for a few seconds²⁵. Similarly, for estimating the orientation of an inertial sensor attached to the body, pose calibration methods, including the N-pose (standing posture with arms stretched vertically downwards) and the T-pose (standing posture with arms extended horizontally perpendicular to the body), are widely used before motion measurement^{26,27}. There have also been suggestions to calibrate the orientation estimation through postural constraints during movements^{28,29}. However, pose calibration can sometimes cause the estimation accuracy to depend on the user's body parameters²⁷, and often interferes with a natural golf swing. Several studies have reported developing and applying filters for the estimation of orientation through the fusion of acceleration, angular velocity, and geomagnetic signals. Kalman filter-based methods have been applied to estimate the orientation of sensors attached to lower limbs and waist during walking^{30–32}. In addition, Mahony filter³³, and Madgwick filter³⁴ have been suggested and are widely used. However, the corrective effect of these filter on golf swing movements, which are characterized by large acceleration changes over short periods, is limited²⁷ due to the need for periodicity and convergence conditions for filter implementation³⁵. Recently, studies have reported the application of machine learning techniques to extract feature points for motion recognition in various activities, including walking³⁶, running³⁷, golf³⁸, tennis³⁹, volleyball⁴⁰, and cross-country⁴¹. Zimmermann et al. used CNNs and Long Short-Term Memory (LSTM) to estimate the alignment between IMUs and body segments during walking⁴². Though not a case of estimating sensor orientation in the ground-fixed coordinate, it is noteworthy because it demonstrates the possibility of extracting information about sensor direction from inertial sensor signals using convolutional neural networks.

The third issue to enhance the tracking accuracy is to correct the inherent drift error in swing trajectory estimates. The causes of drift errors that occur in the integration process of acceleration and angular velocity from inertial sensors include the accumulation of sensor noise such as bias, sensor alignment errors, among others, which increase proportionally with time. Specifically, golf swings, with their fast motion and wide 3D rotation, have been found to produce substantial trajectory tracking errors, often in the range of 30 to 60 centimeters¹¹. In previous research monitoring walking or running activities based on inertial sensors, drift errors were corrected using the features of motion such as ground contact and periodicity. For instance, during walking, the foot's contact with the ground creates a recurring kinematic feature where vertical speed and position become zero. The Zero Velocity Update (ZUPT) method, which periodically updates the speed to zero at the point of ground contact, is widely used^{30,43}. Abdulrahim et al. corrected drift errors by applying a Kalman filter based on the gravitational acceleration information during the stance phase⁴⁴. Kose et al. adjusted the drift error in stride calculation by using the repeated speed at each gait cycle³¹. However, golf swings, unlike walking or running, lack repetitive actions such as ground contact, necessitating the development of novel methods to correct integration errors. Many studies on golf swing mechanics have identified recurring kinematic features among golfers, including the coordination of multi-joint motion and sequential rotations of body segments during swings^{7,8,45–51}. It is worth to examine whether the observed swing kinematics could be used to mitigate drift errors in swing trajectories.

In this study, we addressed two technical issues associated with enhancing the accuracy of golf swing trajectories estimated using a wrist-worn IMU: orientation estimation and drift error reduction. To achieve this, we exploited the kinematic characteristics of golf swing incorporating with machine learning. Specifically, we proposed a method to estimate the sensor's orientation by extracting information of coordinate rotation embedded in the IMU data during a natural swing, without the need for the golfer to perform any pre-calibration actions

such as N-pose or T-pose. We then proposed a drift reduction method by applying the kinematic characteristics of the upper limb during a golf swing. Finally, we quantitatively compared the accuracy of the swing's wrist trajectories as estimated by a single inertial sensor, applying both proposed techniques.

Methods

We proposed solutions to two technical issues necessary for enhancing the accuracy of wrist trajectory tracking during a golf swing using a wrist-worn inertial sensor. The first step in calculating the wrist trajectory involves the segmentation of the main golf swing events from the sensor signal. This step should be followed by the conversion of the relative coordinate frame of the wrist-worn sensor into the ground-fixed absolute coordinate frame. Finally, the removal of the drift error from the wrist trajectory, which results from the integration of the acceleration signal, should be conducted. The two solutions proposed and verified herein are: firstly, to estimate the sensor orientation that transform the relative coordinates into absolute ones without the need for additional sensors or calibration actions; and secondly, to reduce the drift errors arising from the integration of the sensor data.

Experiment

Twenty male right-handed golfers, with an average age of 41.2 ± 9.1 years, height 175.4 ± 6.9 cm, and weight 79.9 ± 13.4 kg, participated in data collection. To test the effectiveness of our proposed trajectory correction method with different swing patterns, we collected data from both professional and amateur golfers using a driver and a 7-iron. Nine professional golfers were members of the Korea Golf Association, and eleven amateur golfers had an average handicap of 15.3 ± 4.3 . Prior to data collection, all participants signed a consent form approved by the KAIST IRB. Participants performed numerous practice swings until they felt comfortable with each club before commencing data collection. During data collection, participants first swung a driver 10 times, then a 7-iron 10 times. The preparation time between swings was approximately 10 s, and swings were initiated at the participant's own pace without specific instruction. Participants took a break for about 5 min before changing clubs. To synchronize the inertial sensor and the motion capture system, a light jump in place was performed prior to each swing.

During a swing, the kinematics of the upper body joints were recorded using both an inertial sensor and a motion capture system (Fig. 1). An IMU (BMA456, BMG250, Bosch Sensortec GmbH, Germany) affixed to the measured acceleration and angular velocity with a measurement range of ± 16 g, ± 2000 dps and a sampling frequency of 200 Hz (Fig. 1). In selecting the IMU, considering the feasibility of device applications such as smartwatches, we took into account the specifications of accelerometers and gyroscopes widely used in various commercial products and studies^{52,53}. Optical markers were placed on the three planes of the inertial sensor (the top of the watch, the medial/lateral sides of the wrist), the left arm including the elbow and shoulder joints, the club, and the ball's position with respect to the club and ground. The positions were then captured using a motion capture camera (Hawk and Eagle, Motion Analysis, USA) with a sampling frequency of 200 Hz and an average 3D residual error of 1.0 ± 0.8 mm. The collected data were filtered at a cut-off frequency of 20 Hz using a Butterworth 10th order low-pass filter. The order and cut-off frequency of the filter were selected to preserve the significant power of the acceleration and angular velocity signal for the fast motion of the golf swing while minimizing the power and peak loss due to filtering^{9,54–57}. Cubic spline interpolation was performed using ten sample data points before and after the clipping segments from the original IMU data for correcting the clipping. Post-processing was conducted to align the time axis of the inertial sensor and motion capture data by matching the peak instances of acceleration signals that occurred during a gentle on-the-spot jump prior to the swing. Out of the total 400 swings—10 trials each for two clubs conducted by 20 participants—we utilized data from 389 swings, excluding 11 instances where data collection errors occurred.

To segment the main sequences of a golf swing from the sensor signal, we employed a machine learning algorithm that trains on time-series data including features capable of identifying these sequences. Four main event points of a golf swing are defined by the movement of the club head: ADD, BST, IMP, and FIN (Fig. 1b). The ADD point is defined as the point where the club head velocity reaches a local minimum just before the backswing. The BST point is identified as the point after the backswing when the club head velocity passes through a local minimum. The IMP point is marked by the point during the downswing when the club head crosses the golf ball's Y-axis position. The FIN point corresponds to the point in the follow-through action when the club head velocity again passes through a local minimum. Following a previous study that showed higher segmentation accuracy when using a BLSTM²¹, this study also used a BLSTM to train on time series data from the wrist-worn IMU to segment the main swing phases (Fig. 1). For validation, the main swing sequences measured by an optical motion capture system were designated as the reference and compared.

Estimation of sensor orientation

For convenience of player, we propose a method to estimate the sensor orientation with respect to the earth coordinate without the need for additional sensors or calibration actions. To compute the wrist trajectory from the data collected by the wrist-attached sensor, it is necessary to identify a quaternion q_s^U that represents the rotation from the sensor's relative coordinate system, or sensor frame S , to the ground-fixed absolute coordinate system, or user frame U (Fig. 1). Initially, the rotation quaternion is specified at the address as $q(t_{ADD})$, which is the starting point of the swing data set. Subsequently, the rotation quaternion, or the sensor orientation for the entire swing segment can be computed by integrating the 3-axis angular velocity measured by the inertial sensor's gyroscope.

Firstly, to specify the rotation quaternion at the address, it is necessary to collect data that includes the sensor's orientation information. This research presumes that consistent sensor orientation can be extrapolated from specific signal segments around the address phase. This presumption is based on the observation that due

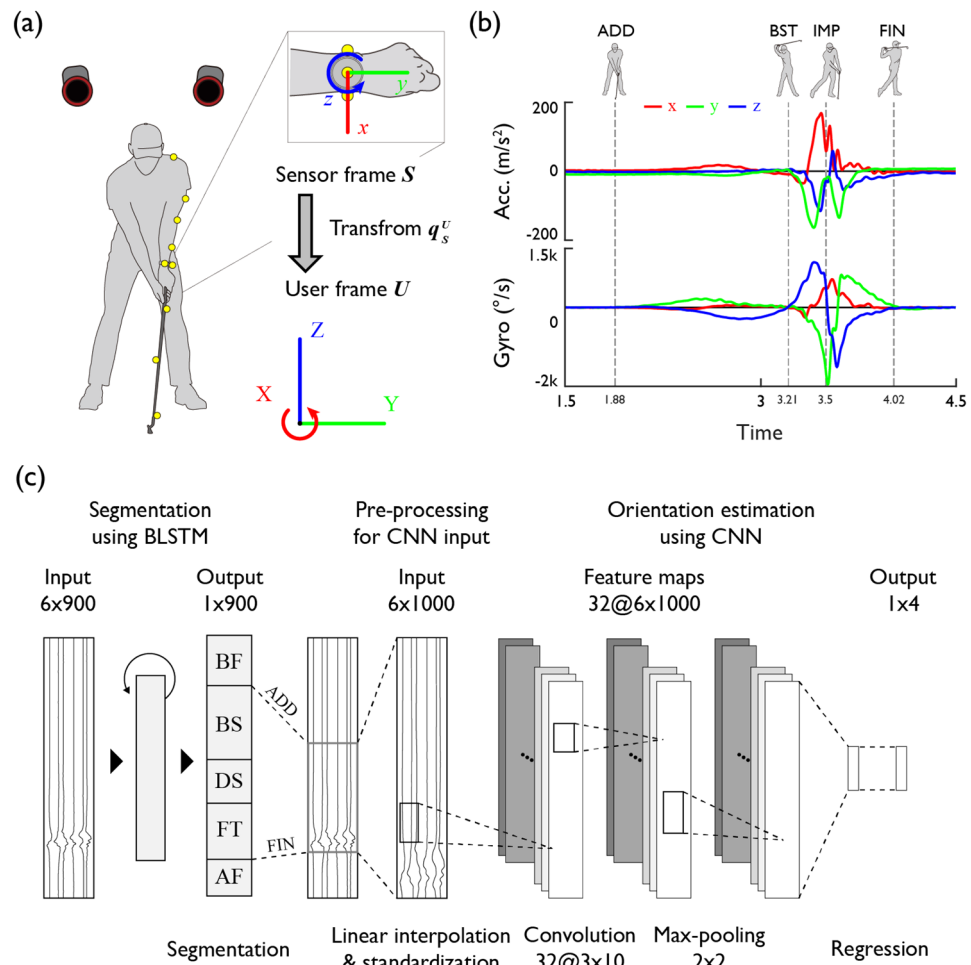


Figure 1. Experimental setup and signal processing overview. **(a)** Defining the sensor orientation using motion capture system and a wrist-worn IMU. **(b)** Acceleration and angular velocity signals of the IMU during the entire swing phases. **(c)** Segmentation, pre-processing, and orientation estimation of the inertial sensor signals.

to physical constraints, the change in the coordinate axis is relatively minor both within and between golfers (inter and intra-player) during the motion preceding and following the address^{58–60}. The correlation between potential features that connote orientation information within the IMU data and the rotation quaternion at the address phase was trained using a CNN. To identify the most effective input data segment for training, we fed various combinations of data, ranging from the pre-address phase to major swing points such as the backswing top, impact, and finish, into the network. This includes static data segments preceding the address phase used in prior studies for orientation correction^{25,27}. To validate the proposed method of sensor orientation estimation, it is necessary to define a reference for calculating absolute error and a baseline for comparison against the single inertial sensor-based orientation estimation method. The reference was defined by the quaternion value calculated by rotating the coordinate system of the inertial sensor, to which three optical markers were attached, to the ground coordinate system, as measured by the motion capture system for the corresponding trial of the subject. The baseline was statistically determined as the average quaternion values at the address point, measured from the motion capture data of all participants excluding the subject in question. Statistical significance for comparison validation was confirmed using a Student's t-test.

The preprocessing and model configuration of the CNN input values for quaternion estimation at the ADD are as Fig. 1. Preprocessing procedures were applied to employ subject-specific swing data as input values for the CNN. To adjust the magnitudes of the six IMU input data to similar levels, the magnitudes were standardized by their means and deviations calculated from other participants. The structure of the CNN consists of two convolutional layers, a max-pooling layer, and a fully connected layer, with each convolutional and max-pooling layer followed by a hyperbolic tangent activation function. The input values are a 6×1000 matrix consisting of 3-axis acceleration and 3-axis angular velocity from the inertial sensor, and the output values are a 1×4 size unit quaternion representing the sensor orientation at the ADD.

We utilized one of the metrics representing quaternion distance as our loss function, ϕ , as

$$\phi(q_{true}, q_{est}) = 1 - |q_{true} \cdot q_{est}| \quad (1)$$

which is the most direct and least computationally intensive approach amongst various metrics for quantifying the distance⁶¹ between the authentic quaternion q_{true} of sensor orientation, ascertained through motion capture, and the estimated quaternion q_{est} , derived from the convolutional neural network. In quaternion notation, the quaternions q and $-q$ denote the same rotation, regardless of their sign. Therefore, we constrained the sensor orientation that serves as the label of the output value of the CNN to reside in the northern hemisphere of the quaternion, where the scalar term is greater than or equal to zero. For the final validation of the trained model's performance, we employed a leave-one-out cross-validation method for the entire dataset, ensuring it did not include data from the subjects used in the training. After excluding the subject in question from the dataset as the test dataset, we randomly selected 90% of the total training dataset for training and assigned the remaining 10% as the validation set. We utilized a validation-based early stopping technique to prevent overfitting. The maximum number of epochs during training was set to 400. The Adam (adaptive moment estimator) optimization method⁶² was used as the optimization method.

Directly following the address, the initial orientation of the IMU at the commencement of a natural golf swing can be established through our previously described orientation estimation technique. Utilizing this initial value, we calculated the orientation of the IMU sensor frame relative to the user frame throughout the entire swing by integrating gyro signals over time. Then, by transforming IMU acceleration measured in the sensor frame into the user frame, we were able to integrate and compute the trajectory of the wrist. As a secondary step after specifying the quaternion at the ADD, the conversion of the coordinate system throughout the entire swing requires computing the rotational quaternion utilizing the 3-axis angular velocity signal captured from the gyroscope. Let the sampling time interval be Δt , and at time t , let the quaternion and angular velocity be $q(t)$, $\omega(t)$, respectively, the quaternion $q(t + 1)$ at the next sampling time is calculated as

$$q(t + 1) = q(t) + \frac{1}{2}(q(t) \otimes \omega(t)) \times \Delta t \quad (2)$$

where \otimes denotes a quaternion product. When calculating the quaternion of the swing interval based on the inertial sensor, drift errors inevitably occur due to the accumulation of noise in the angular velocity of the gyro. To examine the contribution of the proposed orientation estimation method at the ADD to the error reduction during orientation calculation throughout the swing, we made comparisons with scenarios where the orientation specification at the ADD was employed as a reference and baseline. The true sensor orientation across the entire swing phase were determined using an optical motion capture camera system. On the other hand, the baseline was defined as a method that can be calculated using only IMU signals, assuming the availability of reference golf swing data. Specifically, the baseline was defined as the orientation calculated by integrating the IMU angular velocity for the swing phase, with the initial orientation set as the average of the ground truth orientations at the address position of all subjects except the subject in question. The coordinate error was quantified as the rotation angle, which was calculated using the axis-angle representation of the quaternion difference. To ensure a limited range of the error angle θ_{error} within $-\pi < \theta_{error} \leq \pi$, atan2 function was employed.

Reduction of drift error

In order to compute the swing trajectory from a single IMU affixed to the wrist, it is necessary to perform double integration of the acceleration signals for each axis in the absolute coordinate system, as delineated in the preceding section on orientation estimation. Drift errors are inevitable during this integration process due to noise accumulation within the IMU signals. Therefore, this study presents a method aimed at mitigating these drift errors, leveraging the kinematic constraints inherent to wrist movement during a golf swing.

To eliminate the drift error of the velocity that occurs when integrating the acceleration, we applied a constraint that stipulates the wrist speed at the ADD, BST, and FIN approximates zero (Fig. 2). We posited that a time-based linear function could eliminate the drift error occurring during integration, leading us to adopt the subsequent time-based linear correction. The original velocity $v_{i,ori}$ in X-Y-Z ground-fixed coordinate is calculated by the integration of the original acceleration $a_{i,ori}$ as

$$v_{i,ori}(t) = \int_{t_{ADD}}^t a_{i,ori}(t) dt, (t_{ADD} \leq t \leq t_{FIN}, i = X, Y, Z). \quad (3)$$

After applying the time-based linear correction, calibrated velocity $v_{i,Vcal}$ from t_{ADD} to t_{BST} is calculated as

$$v_{i,Vcal}(t) = v_{i,ori}(t) - v_{i,ori}(t_{BST}) \times \frac{t - t_{ADD}}{t_{BST} - t_{ADD}}, (t_{ADD} < t \leq t_{BST}, i = X, Y, Z), \quad (4)$$

and $v_{i,Vcal}$ from t_{BST} to t_{FIN} is calculated as

$$v_{i,Vcal}(t) = v_{i,ori}(t) - v_{i,ori}(t_{BST}) - v_{i,ori}(t_{FIN}) \times \frac{t - t_{BST}}{t_{FIN} - t_{BST}}, (t_{BST} < t \leq t_{FIN}, i = X, Y, Z). \quad (5)$$

To mitigate the drift error that arises when integrating velocity to obtain trajectory, we exploited the feature that the trajectory of the left wrist during a swing closely mirrors a circle on the swing plane^{5,63} (Fig. 2). In particular, a virtual circle was established on the 3D swing plane, and a constraint was implemented stipulating that the swing trajectory remains within this virtual circle. The 3D swing plane was defined by the normal vector \vec{v}_n of the plane that yields the minimum sum of squared orthogonal distances from the wrist trajectory data

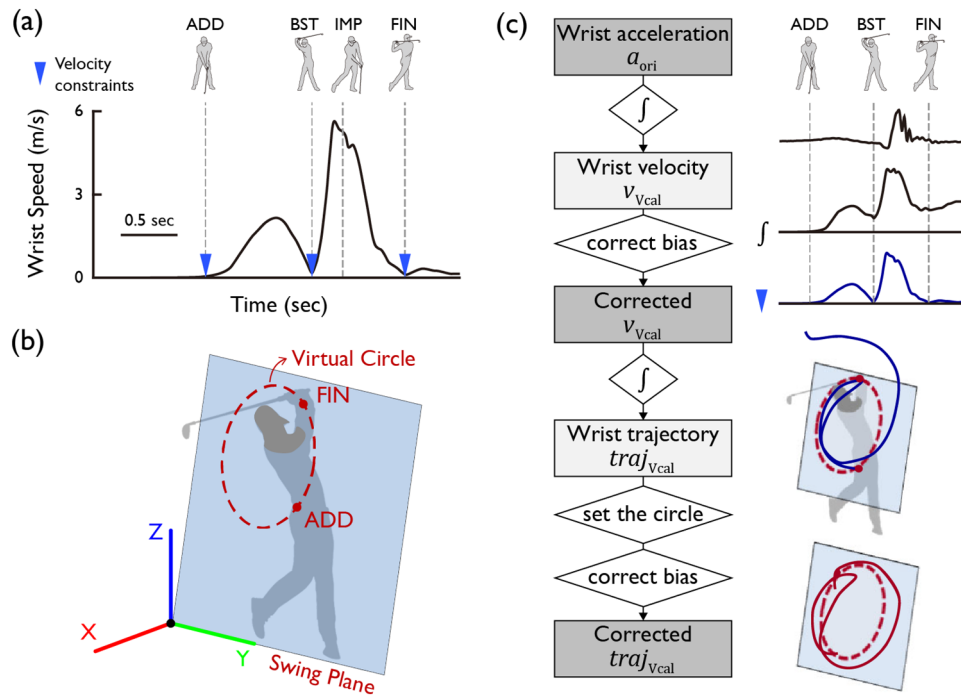


Figure 2. A schematic of the drift error reduction method. (a) Characteristics of the left wrist velocity approximating zero at the ADD, BST, and FIN points during the swing. (b) Characteristics of the left wrist trajectory lying on a virtual circle in the swing plane. (c) Velocity and trajectory correction methods using kinematic constraints of the wrist.

during the backswing, using singular value decomposition. The center c_{circ} and radius r_{circ} of the virtual circle were calculated using the least squares method after projecting the wrist displacement data onto the swing plane. The wrist trajectory $Traj_{i,Vcal}$ was calculated from the corrected velocity $v_{i,Vcal}$ as

$$Traj_{i,Vcal}(t) = \int_{t_{ADD}}^t v_{i,Vcal}(t) dt, (i = X, Y, Z). \quad (6)$$

We then corrected the bias error in the acceleration signal in the x–y–z sensor coordinate system to satisfy the constraint that the displacement at the FIN, where the drift error accumulates the most during integration, is located on the virtual circle (Fig. 2). We can calculate the difference d_{FIN} between $Traj_{i,Vcal}(t_{FIN})$ and the swing plane as

$$d_{FIN} = ((Traj_{i,Vcal}(t_{FIN}) - c_{circ}) \cdot \vec{\nu}_n) \vec{\nu}_n. \quad (7)$$

Then, $Traj_{i,Vcal}(t_{FIN})$ can be projected to the swing plane as

$$r_{cal} = Traj_{i,Vcal}(t_{FIN}) - d_{FIN}. \quad (8)$$

The endpoint of the trajectory can be corrected and located on the virtual circle at ep, calculated as

$$ep = c_{circ} + r_{circ} \left(\frac{r_{cal} - c_{circ}}{\|r_{cal} - c_{circ}\|} \right). \quad (9)$$

From the corrected endpoint ep, the local acceleration bias $a_{j,bias}$ in x–y–z coordinate is estimated as

$$a_{j,bias} = (Traj_{Vcal}(t_{FIN}) - ep)_j \times \frac{1}{\Delta t^2}, (j = x, y, z). \quad (10)$$

By subtracting $a_{j,bias}$ from $a_{j,Vcal}$, which is differentiated by t from $v_{j,Vcal}$ in x–y–z coordinate, $a_{j,Tcal}$ is calculated as

$$a_{j,Tcal}(t) = a_{j,Vcal}(t) - a_{j,bias}, (t_{ADD} \leq t \leq t_{FIN}, j = x, y, z). \quad (11)$$

Finally, the corrected trajectory $Traj_{i,Tcal}$ is calculated such that the endpoint is located on the virtual circle as

$$Traj_{i,Tcal}(t) = \int \int_{t_{ADD}}^t a_{i,Tcal}(t) dt, (t_{ADD} \leq t \leq t_{FIN}, i = X, Y, Z). \quad (12)$$

As a final step, we confirmed the accuracy of the wrist swing trajectory derived from a single IMU by sequentially applying the orientation estimation method coupled with the trajectory correction method proposed in this study. A paired t-test was conducted to verify that the error of our proposed IMU signal processing method was significantly lower than that of existing methods, using the ground truth data from motion capture as the reference.

In this study, we calculated and compared the errors between the proposed method and existing methods based on the values measured by the optical motion capture camera for angle, velocity, and trajectory. For the orientation angle error in the address and entire swing phases, we used the angle between the quaternions representing the rotation of the sensor frame in the user frame, expressed in the axis-angle representation. For velocity and trajectory, we used the mean absolute error (MAE) for each of the X–Y–Z axes, or the 3D vector MAE, as the error metrics.

Results and discussion

Segmentation of sensor data

By applying BLSTM to time-series data from the wrist-worn inertial sensor, we extracted signals corresponding to the golf swing phase, with an average segmentation error of 38 ± 19 ms (mean \pm SD). The errors at the ADD and FIN points (61–69 ms) were approximately five times larger than those at the BST and IMP points (9–15 ms). This is consistent with previous studies due to the low signal-to-noise ratio employed for swing sequence identification at the beginning and the end of the swing phase^{21,64}.

Estimation of sensor orientation

By implementing the proposed sensor orientation estimation method to the wrist-worn IMU data during a natural golf swing, we achieved an error level of 133% compared to the reference and 63% compared to the baseline. At the ADD and throughout the entire swing phase, the mean sensor orientation errors are $7.6 \pm 3.1^\circ$ and $9.5 \pm 3.2^\circ$ respectively (mean \pm SD) (Fig. 3). The sensor orientation error increases over time due to drift error from angular velocity integration. Particularly, the error and deviation escalate dramatically around the moment of impact, where the value of angular velocity increases abruptly (Fig. 3). The findings from the proposed method

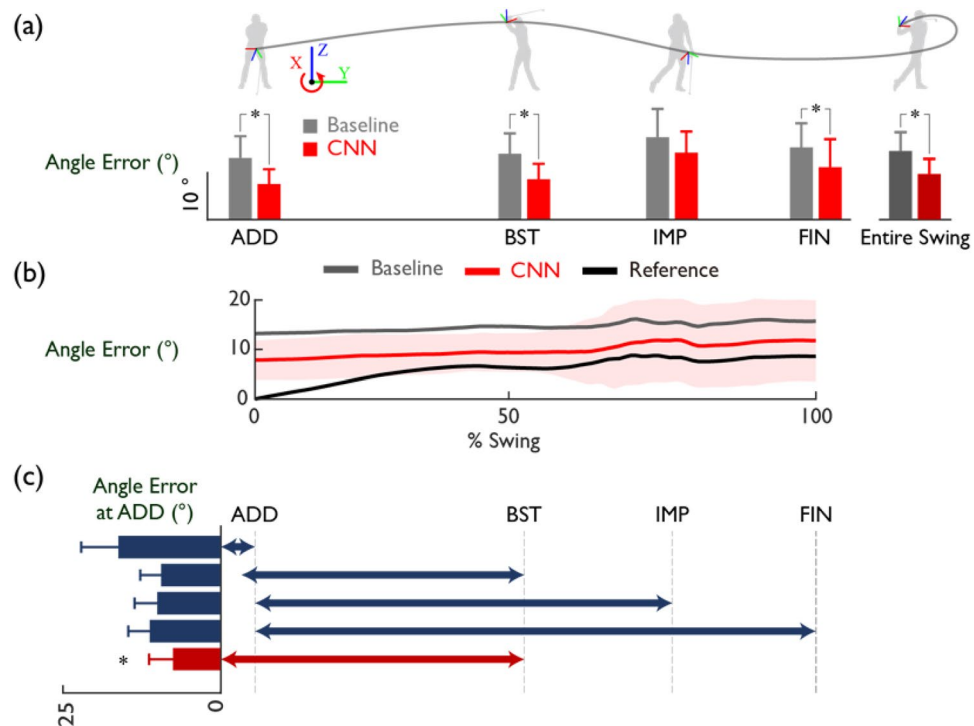


Figure 3. Validation results of the proposed CNN-based sensor orientation estimation method. (a) Angle errors of the orientation estimation at ADD, orientation calculation at BST, IMP, FIN, and for the entire swing phases (* $p < 0.05$). (b) Comparison of orientation errors in the entire swing phases based on different methods for orientation estimation at ADD. The shaded area represents the standard deviation of the CNN method. (c) Comparison of orientation estimation errors for ADD based on different input ranges of CNN. The range before ADD is 100 ms in length (* $p < 0.05$ compared to other methods).

reveal a similar degree of error to those found in the previous research that applied widely used calibration poses by the subjects such as the N-pose and T-pose²⁶. In this study, we did not perform orientation calibration using N-pose or T-pose data, which seems to have limitations in applying to the actual golf field, because our ultimate goal was to overcome the technical hurdles of monitoring swing trajectory using smartwatches during natural golf play in the field. However, similar to the N-pose and T-pose calibration method, which utilizes known orientation information during static calibration movements for IMU orientation estimation, this study applied the initial static pose information during address to orientation estimation, achieving a similar level of calibration accuracy as the hand orientation calibration using N-pose and T-pose²⁶. Also, in comparison with several studies that used inertial sensors to estimate orientation or joint angles (Table 1), our approach displays an error level of similar magnitude.

It is worth noting that our proposed method demonstrated the feasibility of correcting the orientation of an IMU sensor for a fast and wide range of 3D rotational motion like golf swing. The maximum acceleration and angular velocity observed in the wrist-hand during the golf swings measured in this study were about $111 \pm 31 \text{ m/s}^2$ and $1627 \pm 230^\circ/\text{s}$, respectively. These are considerably faster than the dynamic conditions used for previous studies regarding IMU orientation correction such as $5^\circ/\text{s}$ ³⁴, $180\text{--}360^\circ/\text{s}$ ³⁵, $110\text{--}240^\circ/\text{s}$ ⁷⁰, $800\text{--}970^\circ/\text{s}$ ⁷¹. Furthermore, the rotation of the wrist during golf swing demonstrates a wide 3D rotational motion ranged from 150° to 350° in the x–y–z axes. Contrarily, previous investigations into IMU-based motion tracking have predominantly focused on actions such as walking, jogging, and squatting, which exhibit a rotational motion span of about 10° to 60° across each respective axis^{42,67–69}. Fast movements with wide 3D rotation measured with an IMU result in large measurement and the drift error²⁷. Despite the challenges, we successfully estimated the sensor orientation with an error level comparable to those of previous studies, highlighting the effectiveness of our proposed method. The satisfactory calibration results of the IMU orientation during natural golf swings using the CNN suggest that features related to coordinate orientation information can be derived from the time-series data of a wrist-worn IMU. Meanwhile, we adopted a quaternion integration method (Eq. 2) for calculating sensor orientation based on angular velocity from IMU, which is the simplest and computationally cost-effective method and has been widely used in previous studies^{34,72,73}. On the other hand, there have been reports of cases where the orientation error was reduced by applying higher-order integration methods such as the fourth-order Runge–Kutta approach to dynamic state⁷⁴. Therefore, it would be meaningful to conduct future studies that combine the error reduction method proposed in this study with higher-order integration methods to reduce the swing trajectory estimation error of high-speed movements such as golf swings.

One thing to consider when evaluating the results of this study is the potential error in the orientation training data. The orientation values used as ground truth for training the CNN model for orientation estimation were measured using three optical markers attached to a watch-shaped wearable device. According to Yang et al., the static angle error calculated from closely spaced markers (13–24 mm apart) is approximately $0.21\text{--}0.39^\circ$ ⁷⁵. In this study, the average distance between the optical markers fixed on the watch was approximately $69.2 \pm 2.3 \text{ mm}$, which is larger than the spacing in the previous study. Therefore, the error caused by interference from closely spaced markers is likely to be similar to or lower than that in the previous study. However, even assuming that such an error occurs, the average error improvement achieved by the proposed orientation estimation method in this study is 4.5° . Therefore, it can be said that the statistical significance of this estimation is maintained even when considering the error caused by closely spaced markers.

It is interesting to note that using orientation information from the dynamic phase between address and backswing top was more effective for orientation estimation than using only the static address orientation information (Fig. 3). The most effective IMU data for training the CNN to estimate sensor orientation at the ADD includes both the static motion data prior to the ADD and the dynamic data up to the BST as illustrated in Fig. 3. Similar to static IMU calibration poses such as the N-pose and T-pose, gravitational acceleration is used to estimate orientation in the Z-axis when IMU data during the static motion period is input into the CNN. Nonetheless, this segment's limited acceleration information on the X and Y axes hinders the calibration of their corresponding orientation, leading to a relatively lower calibration accuracy. The addition of the data segment from the ADD to the BST into the CNN training enhances calibration accuracy by providing extra information about the X–Y–Z-axis orientation. However, the estimation error rises when downswing data, characterized by a dramatic change in wrist speed direction, is included. This suggests that the most effective orientation calibration employs data from phases exhibiting comparatively consistent and smooth wrist coordinate system rotation. It is also noteworthy that by learning the orientation information of the IMU during someone else's address, the subject can calibrate the orientation of the inertial sensor with high accuracy without performing any prior calibration movements. This implies that there are common features in the IMU signal collected from the address to the

Author	Ueda ⁶⁵	Falbriard ⁶⁶	Zimmermann ⁴²	Adamowicz ⁶⁷	McGrath ⁶⁸	Shin ⁶⁹
Angle error	11° per axis	5–9° standard deviation	8–21° per axis	8–12°	4.3–14.5° per axis	6–8°
Sensor	1 IMU	1 IMU	7 IMUs	8 IMUs	8 IMUs	13 IMUs
Initial cal	Mocap	standing	N-pose	standing	cal. motion	none
Motion	golf swing	running	walking	walking	walking	various

Table 1. Prior studies on orientation estimation and calibration of IMUs in various domains of human motion monitoring. *In most cases, especially when using a small number of sensors, specific actions for the initial calibration are needed.

backswing top of the golf swing that are necessary for orientation estimation. However, it can also be interpreted that the swing data of the golfers who participated in this study had high consistency. In this case, if there is a large variation in swing motion between golfers of different skill levels, the accuracy of the calibration method proposed in this study may decrease and further consideration is needed.

Training the CNN model with a combined dataset encompassing swing data from two different subject groups and two types of clubs yielded lower estimation errors than training the model with each group separately (Table 2). Previous studies have noted between-club differences for golf swing kinematics^{76,77}, and discrepancies have also been observed in swing maneuvers between professional and amateur golfers^{78–80}. Nonetheless, when we separately divided swing samples generated with a driver and a 7-iron for training and validation, the orientation estimation error at the address position exhibited greater average discrepancies ($8.6 \pm 4.4^\circ$ and $9.6 \pm 5.2^\circ$ respectively), compared to the approach of merging the swing datasets from both clubs for training. One potential explanation for this could be the existence of common features in the wrist-worn IMU signals that are valuable for orientation estimation training of the CNN, regardless of the variations across subject groups and club types. Another plausible explanation, and a limitation of our study, is that the data volume used for CNN training might have been insufficient to accurately contrast calibration performance across different subject groups and clubs. The roughly 200 swing trials conducted for each club in this study may not provide an adequately large dataset to ensure the convergence of the CNN model. Du et al. have demonstrated that even within a data sample range of 1,000 to 2,000, a simple CNN model with linear activation functions can consistently decrease in error⁸¹. Consistent with prior studies utilizing CNN models^{82,83}, we anticipate that incorporating additional swing data into training could enhance accuracy and enable the comparison of calibration results, which may vary by golf expertise or club types.

Reduction of drift error

We confirmed the validity of the two assumptions set for wrist trajectory correction: zero velocity approximation and the circular trajectory of wrist. Our proposed method for reducing drift error contributed to a significant enhancement in wrist trajectory accuracy. The velocities at the ADD, BST, and FIN relative to the maximum swing speed were $0.9 \pm 1.2\%$, $4.8 \pm 1.9\%$, and $2.1 \pm 0.9\%$ respectively, and are substantially approximating to zero. The R-squared value between the wrist trajectory from the motion capture and the fitted virtual circle was 0.984 ± 0.007 across the whole swing phase, confirming the validity of the circular trajectory assumption (Table 3). Utilizing the proposed trajectory estimation method led to a significant reduction ($p = 3e-5$) of more than 40% in the absolute velocity and trajectory errors, from 0.76 ± 0.22 m/s to 0.42 ± 0.10 m/s, and from 0.39 ± 0.14 m to 0.21 ± 0.08 m, respectively (Fig. 4). This outcome aligns with previous studies^{30,31} that mitigated integration errors through the application of ground contact points of the foot during walking. This suggests that the kinematic properties of motion can contribute to enhancing the accuracy of IMU-based motion monitoring.

The proposed wrist trajectory estimation method considerably improved wrist trajectory estimation despite differences in swing patterns between clubs. In the driver swing, the mean absolute trajectory error decreased by approximately 40%, from 0.350 ± 0.129 m to 0.213 ± 0.079 m, and in the 7-iron swing, it decreased by approximately 52%, from 0.424 ± 0.162 m to 0.203 ± 0.077 m (Table 4). Prior to the application of the drift error reduction method, the 7-iron swing showed a larger mean absolute error in both speed and trajectory in comparison with the driver swing. However, after error correction, no considerable differences were found in both speed

Swing event points		ADD	BST	IMP	FIN	Entire swing
Total		$7.6 \pm 3.1^\circ$	$8.5 \pm 3.3^\circ$	$14.1 \pm 4.5^\circ$	$11.1 \pm 5.9^\circ$	$9.5 \pm 3.2^\circ$
Skill level	Professional	$9.4 \pm 3.9^\circ$	$10.1 \pm 4.0^\circ$	$15.0 \pm 2.8^\circ$	$13.2 \pm 5.1^\circ$	$11.3 \pm 3.5^\circ$
	Amateur	$9.7 \pm 3.8^\circ$	$10.4 \pm 3.1^\circ$	$12.6 \pm 5.0^\circ$	$13.6 \pm 5.6^\circ$	$11.3 \pm 3.6^\circ$
Club	Driver	$8.6 \pm 4.4^\circ$	$9.1 \pm 4.5^\circ$	$14.9 \pm 5.9^\circ$	$10.6 \pm 5.7^\circ$	$10.0 \pm 3.9^\circ$
	7-iron	$9.6 \pm 5.2^\circ$	$10.8 \pm 4.9^\circ$	$15.4 \pm 6.3^\circ$	$13.6 \pm 7.5^\circ$	$11.9 \pm 5.0^\circ$

Table 2. Comparison of sensor orientation estimation and calculation results for different groups of training datasets in CNN, with mean values and standard deviations (mean \pm SD) (* $p < 0.05$ compared to other groups).

Swing phases		Backswing	Downswing	Follow-through	Entire swing
Total		0.991 ± 0.005	0.944 ± 0.028	0.957 ± 0.023	0.984 ± 0.007
Skill level	Professional	0.992 ± 0.002	0.960 ± 0.016	0.949 ± 0.020	0.984 ± 0.005
	Amateur	0.990 ± 0.006	0.930 ± 0.028	0.964 ± 0.024	0.984 ± 0.009
Club	Driver	0.991 ± 0.005	0.927 ± 0.038	0.951 ± 0.025	0.981 ± 0.008
	7-iron	0.992 ± 0.004	0.961 ± 0.019	0.962 ± 0.023	0.986 ± 0.007

Table 3. Comparison of the circular trajectory assumption quantitatively using R-squared value between the wrist trajectory obtained from the motion capture and the fitted virtual circle for different groups, with mean values and standard deviations (mean \pm SD).

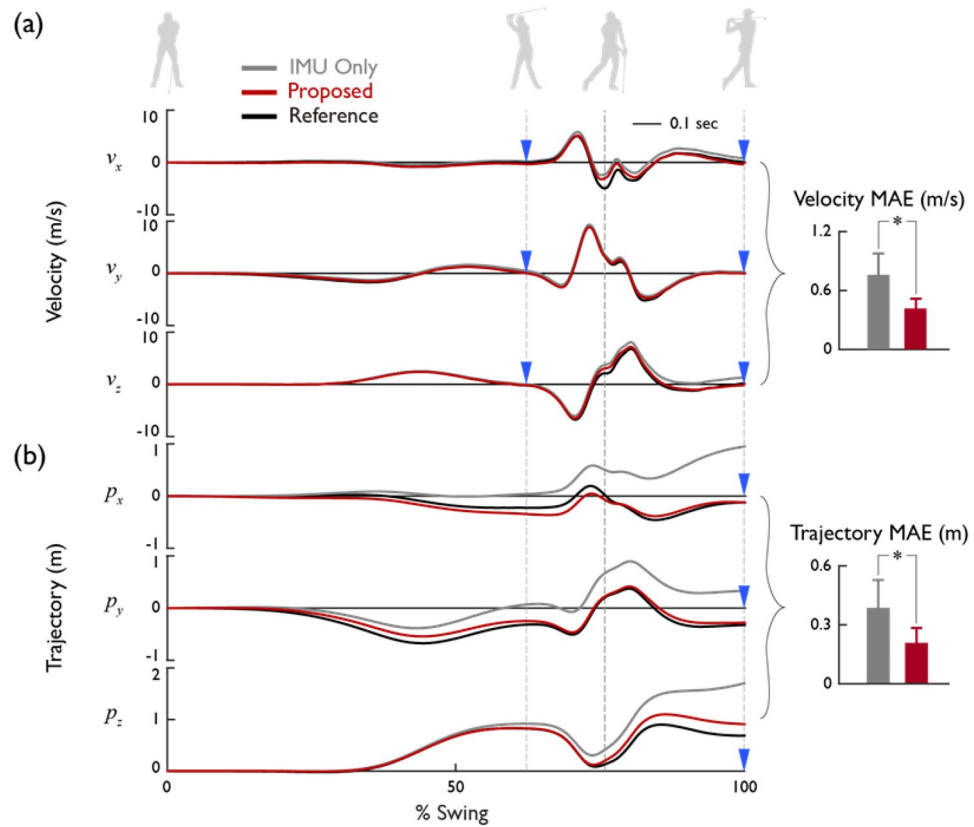


Figure 4. Validation results of the proposed drift error reduction method. A comparison of the (a) velocity and (b) trajectory calculations using only IMU and applying the proposed method for a representative swing trial, considering the ground-fixed X, Y, and Z axes. Blue inverted triangles indicate the points where kinematic characteristics are reflected. The bar graph compares the mean absolute error values based on the norm values (* $p < 0.05$).

methods		Velocity MAE (m/s)		Trajectory MAE (m)	
		IMU only	Proposed	IMU only	Proposed
Total		0.760 ± 0.217	*0.415 ± 0.103	0.387 ± 0.141	*0.208 ± 0.076
Skill level	Professional	0.929 ± 0.164	*0.464 ± 0.101	0.504 ± 0.096	*0.228 ± 0.067
	Amateur	0.621 ± 0.144	*0.376 ± 0.086	0.292 ± 0.090	*0.191 ± 0.078
Club	Driver	0.694 ± 0.212	*0.402 ± 0.088	0.350 ± 0.129	*0.213 ± 0.079
	7-iron	0.826 ± 0.285	*0.428 ± 0.131	0.424 ± 0.162	*0.203 ± 0.077

Table 4. Comparison of velocity and trajectory errors before (IMU only) and after (proposed) applying the suggested drift error reduction method for different groups, with mean values and standard deviations (mean ± SD) (* $p < 0.05$ compared to IMU only).

and trajectory across clubs. The 7-iron swing exhibited a more substantial correction effect as it more closely conformed to the circular approximation assumption of the wrist trajectory in the swing plane (Table 3).

The trajectory estimation method exhibited its most substantial effect around the FIN. The drift error, which accumulates due to the integration process, escalates over time, with a pronounced increase observed near the IMP, where the swing speed is at its maximum. Consequently, the greatest error is shown at the finish of the swing (Fig. 4, Table 5). By incorporating a constraint that posits the wrist trajectory at the FIN to lie on a virtual circle within the swing plane, we were able to effectively rectify the substantial drift error observed at the FIN. The most substantial velocity and trajectory errors were observed along the Y-axis, which is the progression direction of the swing (Table 6). Large errors in the Y-direction may be attributed to the high Y-axis speed near the IMP point and the absence of velocity or trajectory adjustment constraints around the IMP. Therefore, to improve this, additional consideration is needed to ascertain if there is kinematic information that can be utilized for trajectory correction near the IMP.

We proposed an IMU integral error reduction method utilizing kinematic information, such as trajectory changes induced by arm joint movements during a golf swing. In addition, there is a possibility that information

Swing phase	Backswing		Downswing		Follow-through	
Methods	IMU only	Proposed	IMU only	Proposed	IMU only	Proposed
Velocity MAE (m/s)	0.287 ± 0.092	0.270 ± 0.093	0.662 ± 0.247	*0.560 ± 0.142	1.630 ± 0.499	*0.611 ± 0.140
Trajectory MAE (m)	0.119 ± 0.046	0.112 ± 0.042	0.340 ± 0.123	*0.266 ± 0.123	0.863 ± 0.309	*0.343 ± 0.140

Table 5. Comparison of velocity and trajectory errors before (IMU only) and after (proposed) applying the suggested drift error reduction method, based on swing phases, with mean values and standard deviations (mean ± SD) (*p < 0.05 compared to IMU only).

Axis	X		Y		Z	
Methods	IMU only	Proposed	IMU only	Proposed	IMU only	Proposed
Velocity MAE (m/s)	0.349 ± 0.152	*0.184 ± 0.074	0.485 ± 0.149	*0.261 ± 0.080	0.300 ± 0.133	*0.174 ± 0.044
Trajectory MAE (m)	0.178 ± 0.093	*0.079 ± 0.035	0.264 ± 0.129	*0.136 ± 0.072	0.134 ± 0.070	*0.095 ± 0.049

Table 6. Comparison of velocity and trajectory errors before (IMU only) and after (proposed) applying the suggested drift error reduction method, based on X–Y–Z coordinates, with mean values and standard deviations (mean ± SD) (*p < 0.05 compared to IMU only).

that can be used for error correction exists if we analyze the wrist orientation trajectory during the swing, even though it is relatively difficult to visualize. For instance, we suggest, as a potential avenue for future research, the utilization of quantitative characteristics such as the gradual rotation of wrist orientation in the early phase of the backswing or the symmetry around the backswing top, for error reduction.

Validation of the proposed methods

When we combined the orientation estimation and drift error reduction methods proposed in this study, the wrist trajectory error was reduced to 0.168 ± 0.054 m. This demonstrates a significant reduction ($p = 2e-9$) of approximately $82.3 \pm 9.5\%$, compared to the baseline error of 1.094 ± 0.388 m (Table 7). The baseline error was calculated using statistical orientation and simple integration of the IMU signal. Moreover, to quantitatively assess the similarity between the estimated and reference trajectories in 3D space, we calculated the R-squared value to be 0.859 ± 0.081 . This represents a substantial improvement compared to the baseline R-squared value of -0.766 ± 0.313 .

Despite using only single IMU data, the proposed trajectory estimation method demonstrated tracking performance comparable to golf swing tracking methods that additionally utilize multimodal data such as images. The full golf swing trajectory spans approximately 4.4 m, and we estimated the wrist trajectory with an average error of about 17 cm, yielding an error level of about 4% relative to the entire motion range. This error level aligns with those reported in prior golf tracking studies that employed vision sensors like depth or stereo cameras, either independently or in combination with an IMU. Jia et al. reported a wrist trajectory estimation error of 17 cm using a depth camera alone and roughly 10 cm when integrated with an IMU¹¹. Nam et al. demonstrated a club trajectory estimation error of 13.2 cm by fusing data from an IMU and LED attached to the club with information from a ground-installed stereo camera¹⁴. However, Cheon et al. recorded an average error of 7 cm for clubhead trajectory estimation utilizing a single IMU, showcasing a higher trajectory accuracy compared to our study, thus warranting further exploration¹⁸. The single IMU-based trajectory tracking method introduced in this study is noteworthy due to the convenience and data utility it ensures in contrast to video-based tracking techniques.

When compared with prior motion tracking studies using a single inertial sensor, the method proposed in this study effectively eliminated the cumulative error in rapid, non-periodic movements. Previous work on gait tracking employing a single inertial sensor has yielded estimation errors of 6–7%³² and 12–25%⁸⁴ proportional to the range of motions, and errors around 28.1 cm for jumping movements⁸⁵. By computing the foot trajectory during walking via an inertial sensor affixed to the instep, Kitagawa et al. estimated the stride to within an error margin of 5 cm (3–4% of stride length)⁴³. Hao and colleagues estimated stride length and step width with RMS

Methods	Velocity MAE (m/s)		Trajectory MAE (m)	
	IMU only	Proposed	IMU only	Proposed
Total	1.587 ± 0.471	*0.394 ± 0.127	1.094 ± 0.388	*0.168 ± 0.054

Table 7. Estimation errors of wrist swing velocity and trajectory using the baseline method for sensor orientation estimation and simple integration of acceleration (IMU only), and the proposed methods for sensor orientation estimation and drift error reduction in series, with mean values and standard deviations (mean ± SD) (*p < 0.05 compared to IMU only).

errors of 1.14 cm and 0.95 cm respectively, using an inertial sensor attached to the rear of the foot⁸⁶. Cardarelli et al. used an inertial sensor attached to the sacrum to estimate the displacement of the body's center of gravity to within 0.25 cm during treadmill walking³². In the case of gait, the limb movements are coordinated, joint kinematics of many subjects are quite consistent, motions are periodic and under moderate speed, and there are repeated ZUPT moments. As a result, many prior studies employing single IMU-based trajectory tracking have reported high levels of accuracy. However, for golf swing tracking, which has large variability between players, skill levels, and clubs, and involves fast movements over a wide range of 3D rotation, single IMU-based trajectory tracking can yield high errors up to 30–60 cm¹¹ (Fig. 4, Table 7). Taking into account the difficulties inherent in tracking golf swing motions, it is worth highlighting that our study has successfully mitigated tracking errors to a remarkable extent in movements that are rapid, non-periodic, and span a wide 3D rotational range.

We investigated whether the IMU used for measurement accurately measured the rapid kinematic information of the wrist during a golf swing. Among the 389 swings collected in the experiment, it was observed that 150 swings showed clipping around 0.9% of the time during the impact phase within an average swing duration of 2.14 s. To address this, we performed cubic spline interpolation using ten sample data points before and after the clipping segments from the original IMU data to correct the clipping. Through this correction, the peak error between the acceleration and angular velocity from the markers and the IMU decreased from $9.1 \pm 6.4\%$ to $7.4 \pm 5.7\%$ and $16.5 \pm 10.5\%$ to $7.3 \pm 6.3\%$, respectively. To examine whether the use of clipping corrected IMU data affect to the swing trajectory correction method proposed in this study, we performed the trajectory correction using acceleration and angular velocity calculated from motion capture assuming that IMU data without clipping was used. In this case, swing trajectory error was reduced by approximately $78.3 \pm 10.7\%$, which was not statistically significantly different ($p > 0.05$) from the error reduction using the clipping corrected IMU data in Table 7. Therefore, it can be said that the adopted clipping correction method has a limited effect on the main research results of the swing trajectory error reduction proposed in this study.

It is worth to note that the proposed orientation estimation and drift removal methods utilize the characteristic of consistency in swing motion observed across golfers. Therefore, the effectiveness of the proposed trajectory correction method may be reduced for golfers with lower swing consistency than those who participated in this study. However, previous studies by Brown et al.⁸⁷, and Glazier et al.⁸⁸ have reported that while golf swings exhibit high intra-individual (within-person swing) consistency, there is also large inter-individual (between-person) variability in the swings of even high-skill level golfers, making it difficult to find a common optimal technique. Glazier et al.⁸⁸, Tucker⁸⁹, and Langdown et al.⁶⁰ argued that there is a lack of research on the criteria for individual and intra-individual movement variability in golf swings and whether this is beneficial or detrimental to swing performance, and that more research is needed on this complex topic. Therefore, future studies with swing data from golfers with different skill levels and swing styles are needed to investigate the potential for generalizing the results of this study.

In this study, we successfully tackled technical challenges to enhance the accuracy and convenience of golf swing tracking using a wrist-worn IMU. By harnessing observed kinematic characteristics from golfers, including consistent and continuous sensor coordinate rotation around the ADD, and by incorporating machine learning, we were able to estimate sensor orientation with error levels comparable to previous studies. This was achieved without the need for pre-calibration poses or additional sensor information. Moreover, we substantially reduced the inherent drift error typically associated with IMU-based trajectory estimation, through the application of upper limb swing kinematics within a 3-dimensional swing plane. Our research thus introduces a novel signal processing method for tracking rapid, wide-ranging motions, such as a golf swing, while maintaining user convenience. Our results could impact the burgeoning field of daily motion monitoring for health care, especially with the increasing prevalence of wearable devices like smartwatches.

Data availability

The datasets generated during and/or analyzed during the current study are not publicly available due to the reason that they involve handling experimental data with human subjects, but are available from the corresponding author on reasonable request.

Received: 2 June 2023; Accepted: 17 April 2024

Published online: 22 April 2024

References

- Hume, P. A., Keogh, J. & Reid, D. The role of biomechanics in maximising distance and accuracy of golf shots. *Sport. Med.* **35**, 429–449 (2005).
- Chu, Y., Sell, T. C. & Lephart, S. M. The relationship between biomechanical variables and driving performance during the golf swing. *J. Sports Sci.* **28**, 1251–1259 (2010).
- Kim, S. E. et al. Small changes in ball position at address cause a chain effect in golf swing. *Sci. Rep.* **11**, 2694 (2021).
- Neal, R., Lumsden, R., Holland, M. & Mason, B. Body segment sequencing and timing in golf. *Int. J. Sports Sci. Coach.* **2**, 25–36 (2007).
- Nesbit, S. M. & McGinnis, R. S. Kinetic constrained optimization of the golf swing hub path. *J. Sport. Sci. Med.* **13**, 859–873 (2014).
- MacKenzie, S. J. & Spriggins, E. J. A three-dimensional forward dynamics model of the golf swing. *Sport. Eng.* **11**, 165–175 (2009).
- Spriggins, E. J. & Mackenzie, S. J. Examining the delayed release in the golf swing using computer simulation. *Sport. Eng.* **5**, 23–32 (2002).
- Kenny, I. C., McCloy, A. J., Wallace, E. S. & Otto, S. R. Segmental sequencing of kinetic energy in a computer-simulated golf swing. *Sport. Eng.* **11**, 37–45 (2008).
- Anderson, B. C. *Speed Generation in the Golf Swing: An Analysis of Angular Kinematics, Kinetic Energy and Angular Momentum in Player Body Segments* (2007).
- Chun, S. et al. A sensor-Aided self coaching model for uncocking improvement in golf swing. *Multimed. Tools Appl.* **72**, 253–279 (2014).

11. Jia, H., Hu, J. & Hu, W. SwingNet: Ubiquitous fine-grained swing tracking framework via stochastic neural architecture search and adversarial learning. *Proc. ACM Interact. Mobile Wearable Ubiquitous Technol.* **5**, 1–21 (2021).
12. Park, S., Chang, J. Y., Jeong, H., Lee, J.-H. & Park, J.-Y. Accurate and efficient 3D human pose estimation algorithm using single depth images for pose analysis in golf. In *2017 IEEE Conference on Computer Vision and Pattern Recognition Workshops (CVPRW) 2017-July*, 105–113 (IEEE, 2017).
13. Ko, K.-R. & Pan, S. B. CNN and bi-LSTM based 3D golf swing analysis by frontal swing sequence images. *Multimed. Tools Appl.* **80**, 8957–8972 (2021).
14. Nam, C. N. K., Kang, H. J. & Suh, Y. S. Golf swing motion tracking using inertial sensors and a stereo camera. *IEEE Trans. Instrum. Meas.* **63**, 943–952 (2014).
15. Kim, Y. J., Kim, K. D., Kim, S. H., Lee, S. & Lee, H. S. Golf swing analysis system with a dual band and motion analysis algorithm. *IEEE Trans. Consum. Electron.* **63**, 309–317 (2017).
16. King, K., Yoon, S. W., Perkins, N. C. & Najafi, K. Wireless MEMS inertial sensor system for golf swing dynamics. *Sens. Actuators A* **141**, 619–630 (2008).
17. Jensen, U. *et al.* An IMU-based mobile system for golf putt analysis. *Sport. Eng.* **18**, 123–133 (2015).
18. Cheon, M., Khuyagbaatar, B., Yeom, J.-H. & Kim, Y. H. Analysis of swing tempo, swing rhythm, and functional swing plane slope in golf with a wearable inertial measurement unit sensor. *J. Mech. Sci. Technol.* **34**, 3095–3101 (2020).
19. Kooyman, D. J., James, D. A. & Rowlands, D. D. A feedback system for the motor learning of skills in golf. *Procedia Eng.* **60**, 226–231 (2013).
20. Hsu, Y. *et al.* Golf swing motion detection using an inertial-sensor-based portable instrument. *2016 IEEE Int. Conf. Consum. Electron.* 1–2 (2016). <https://doi.org/10.1109/ICCE-TW.2016.7521016>.
21. Kim, M. & Park, S. Golf swing segmentation from a single IMU using machine learning. *Sensors* **20**, 4466 (2020).
22. Yi, C. *et al.* Estimating three-dimensional body orientation based on an improved complementary filter for human motion tracking. *Sensors* **18**, 3765 (2018).
23. Sabatini, A. M. Quaternion-based strap-down integration method for applications of inertial sensing to gait analysis. *Med. Biol. Eng. Comput.* **43**, 94–101 (2005).
24. Pasciuto, I. *et al.* How angular velocity features and different gyroscope noise types interact and determine orientation estimation accuracy. *Sensors* **15**, 23983–24001 (2015).
25. Walmsley, C. P. *et al.* Measurement of upper limb range of motion using wearable sensors: A systematic review. *Sport. Med. Open* **4**, 53 (2018).
26. Robert-Lachaine, X., Mecheri, H., Larue, C. & Plamondon, A. Accuracy and repeatability of single-pose calibration of inertial measurement units for whole-body motion analysis. *Gait Posture* **54**, 80–86 (2017).
27. Schepers, M., Giuberti, M. & Bellusci, G. Xsens MVN: Consistent Tracking of human motion using inertial sensing. *Xsens Technol.* <https://doi.org/10.13140/RG.2.2.22099.07205> (2018).
28. Cooper, G. *et al.* Inertial sensor-based knee flexion/extension angle estimation. *J. Biomech.* **42**, 2678–2685 (2009).
29. Seel, T., Raisch, J. & Schauer, T. IMU-based joint angle measurement for gait analysis. *Sensors* **14**, 6891–6909 (2014).
30. Rebula, J. R., Ojeda, L. V., Adamczyk, P. G. & Kuo, A. D. Measurement of foot placement and its variability with inertial sensors. *Gait Posture* **38**, 974–980 (2013).
31. Köse, A., Cereatti, A. & Della Croce, U. Bilateral step length estimation using a single inertial measurement unit attached to the pelvis. *J. Neuroeng. Rehabil.* **9**, 9 (2012).
32. Cardarelli, S. *et al.* Single IMU displacement and orientation estimation of human center of mass: A magnetometer-free approach. *IEEE Trans. Instrum. Meas.* **69**, 5629–5639 (2020).
33. Mahony, R., Hamel, T. & Pfimlin, J.-M. Nonlinear complementary filters on the special orthogonal group. *IEEE Trans. Automat. Contr.* **53**, 1203–1218 (2008).
34. Madgwick, S. O. H., Harrison, A. J. L. & Vaidyanathan, R. Estimation of IMU and MARG orientation using a gradient descent algorithm. In *2011 IEEE International Conference on Rehabilitation Robotics* 1–7 (IEEE, 2011). <https://doi.org/10.1109/ICORR.2011.5975346>.
35. Ricci, L., Taffoni, F. & Formica, D. On the orientation error of IMU: Investigating static and dynamic accuracy targeting human motion. *PLoS ONE* **11**, e0161940 (2016).
36. Martinez-Hernandez, U., Rubio-Solis, A. & Dehghani-Sanij, A. A. Recognition of walking activity and prediction of gait periods with a CNN and first-order MC strategy. In *2018 7th IEEE International Conference on Biomedical Robotics and Biomechanics (Biorob) 2018* 897–902 (IEEE, 2018).
37. Tan, T., Strout, Z. A. & Shull, P. B. Accurate impact loading rate estimation during running via a subject-independent convolutional neural network model and optimal IMU placement. *IEEE J. Biomed. Heal. Inform.* <https://doi.org/10.1109/JBHI.2020.3014963> (2020).
38. Jiao, L., Wu, H., Bie, R., Umek, A. & Kos, A. Multi-sensor golf swing classification using deep CNN. *Procedia Comput. Sci.* **129**, 59–65 (2018).
39. Anand, A., Sharma, M., Srivastava, R., Kaligounder, L. & Prakash, D. Wearable Motion sensor based analysis of swing sports. In *2017 16th IEEE International Conference on Machine Learning and Applications (ICMLA) 2017* 261–267 (IEEE, 2017).
40. Kautz, T. *et al.* Activity recognition in beach volleyball using a Deep Convolutional Neural Network. *Data Min. Knowl. Discov.* **31**, 1678–1705 (2017).
41. Rassem, A., El-Beltagy, M. & Saleh, M. *Cross-Country Skiing Gears Classification using Deep Learning* 1–14 (2017).
42. Zimmermann, T., Taetz, B. & Bleser, G. IMU-to-segment assignment and orientation alignment for the lower body using deep learning. *Sensors* **18**, 302 (2018).
43. Kitagawa, N. & Ogihara, N. Estimation of foot trajectory during human walking by a wearable inertial measurement unit mounted to the foot. *Gait Posture* **45**, 110–114 (2016).
44. Abdulrahim, K., Moore, T., Hide, C. & Hill, C. Understanding the performance of zero velocity updates in MEMS-based pedestrian navigation. *Int. J. Adv. Technol.* **5**, 53–60 (2014).
45. Meister, D. W. *et al.* Rotational biomechanics of the elite golf swing: benchmarks for amateurs. *J. Appl. Biomech.* **27**, 242–251 (2011).
46. Cooper, J. M., Bates, B. T., Bedi, J. & Scheuchenzuber, J. Kinematic and kinetic analysis of the golf swing. In *Biomechanics IV* 298–305 (Macmillan Education UK, 1974). https://doi.org/10.1007/978-1-349-02612-8_44.
47. Neal, R. J. & Wilson, B. D. 3D Kinematics and kinetics of the golf swing. *Int. J. Sport Biomech.* **1**, 221–232 (1985).
48. Burden, A. M., Grimshaw, P. N. & Wallace, E. S. Hip and shoulder rotations during the golf swing of sub-10 handicap players. *J. Sports Sci.* **16**, 165–176 (1998).
49. Tinmark, F., Hellström, J., Halvorsen, K. & Thorstensson, A. Elite golfers' kinematic sequence in full-swing and partial-swing shots. *Sport. Biomech.* **9**, 236–244 (2010).
50. Coleman, S. G. S. & Rankin, A. J. A three-dimensional examination of the planar nature of the golf swing. *J. Sports Sci.* **23**, 227–234 (2005).
51. Lamb, P. F. & Glazier, P. S. The sequence of body segment interactions in the golf swing. *Routledge Int. Handb. Golf Sci.* <https://doi.org/10.4324/9781315641782-4> (2018).
52. Rana, M. & Mittal, V. Wearable sensors for real-time kinematics analysis in sports: A review. *IEEE Sens. J.* **21**, 1187–1207 (2021).
53. Kim, S. E. *et al.* Validation of inertial measurement units for analyzing golf swing rotational biomechanics. *Sensors* **23**, 8433 (2023).

54. Sung, J. *et al.* Prediction of lower extremity multi-joint angles during overground walking by using a single IMU with a low frequency based on an LSTM recurrent neural network. *Sensors* **22**, 53 (2021).
55. Esser, P., Dawes, H., Collett, J. & Howells, K. IMU: Inertial sensing of vertical CoM movement. *J. Biomech.* **42**, 1578–1581 (2009).
56. Choi, A., Jung, H. & Mun, J. H. Single inertial sensor-based neural networks to estimate COM-COP inclination angle during walking. *Sensors* **19**, 2974 (2019).
57. Day, E. M., Alcantara, R. S., McGeehan, M. A., Grabowski, A. M. & Hahn, M. E. Low-pass filter cutoff frequency affects sacral-mounted inertial measurement unit estimations of peak vertical ground reaction force and contact time during treadmill running. *J. Biomech.* **119**, 110323 (2021).
58. Langdown, B. L., Bridge, M. W. & Li, F.-X. Address position variability in golfers of differing skill level. *Int. J. Golf Sci.* **2**, 1–9 (2013).
59. Langdown, B. L., Bridge, M. W. & Li, F.-X. Impact position variability in golfers of differing skill level. *Int. J. Golf Sci.* **2**, 142–151 (2013).
60. Langdown, B. L., Bridge, M. & Li, F. X. Movement variability in the golf swing. *Sport. Biomech.* **11**, 273–287 (2012).
61. Huynh, D. Q. Metrics for 3D rotations: Comparison and analysis. *J. Math. Imaging Vis.* **35**, 155–164 (2009).
62. Kingma, D. P. & Ba, J. Adam: A Method for Stochastic Optimization. *3rd Int. Conf. Learn. Represent. ICLR 2015—Conf. Track Proc.* (2014).
63. Lee, C. & Park, S. Estimation of unmeasured golf swing of arm based on the swing dynamics. *Int. J. Precis. Eng. Manuf.* **19**, 745–751 (2018).
64. Mesaros, A., Heittola, T., Eronen, A. & Virtanen, T. Acoustic event detection in real life recordings. In *European Signal Processing Conference* 1267–1271 (2010).
65. Ueda, M., Negoro, H., Kurihara, Y. & Watanabe, K. Measurement of angular motion in golf swing by a local sensor at the grip end of a golf club. *IEEE Trans. Human-Machine Syst.* **43**, 398–404 (2013).
66. Falbriard, M., Meyer, F., Mariani, B., Millet, G. P. & Aminian, K. Drift-free foot orientation estimation in running using wearable IMU. *Front. Bioeng. Biotechnol.* **8**, 65 (2020).
67. Adamowicz, L. *et al.* Validation of novel relative orientation and inertial sensor-to-segment alignment algorithms for estimating 3D hip joint angles. *Sensors* **19**, 5143 (2019).
68. McGrath, T. & Stirling, L. Body-worn IMU-based human hip and knee kinematics estimation during treadmill walking. *Sensors* **22**, 2544 (2022).
69. Shin, S., Li, Z. & Halilaj, E. Markerless Motion Tracking with Noisy Video and IMU Data. *IEEE Trans. Biomed. Eng.* <https://doi.org/10.1109/TBME.2023.3275775> (2023).
70. Cutti, A. G., Giovanardi, A., Rocchi, L. & Davalli, A. A simple test to assess the static and dynamic accuracy of an inertial sensors system for human movement analysis. *Annu. Int. Conf. IEEE Eng. Med. Biol.—Proc.* 5912–5915 (2006). <https://doi.org/10.1109/IEMBS.2006.260705>.
71. Lee, J. & Choi, M. Effect of strapdown integration order and sampling rate on IMU-based attitude estimation accuracy. *Sensors* **18**, 2775 (2018).
72. Valenti, R., Dryanovski, I. & Xiao, J. Keeping a good attitude: A quaternion-based orientation filter for IMUs and MARGs. *Sensors* **15**, 19302–19330 (2015).
73. Harindranath, A. & Arora, M. MEMS IMU sensor orientation algorithms-comparison in a simulation environment. in *2018 International Conference on Networking, Embedded and Wireless Systems (ICNEWS)* 1–6 (IEEE, 2018). <https://doi.org/10.1109/ICNEWS.2018.8904029>.
74. Zebin, T., Scully, P. & Ozanyan, K. B. Inertial sensing for gait analysis and the scope for sensor fusion. *2015 IEEE SENSORS—Proc* 1–8 (2015). <https://doi.org/10.1109/ICSENS.2015.7370262>.
75. Yang, Z., Yan, S., van Beijnum, B.-J.F., Li, B. & Veltink, P. H. Improvement of optical tracking-based orientation estimation by fusing gyroscope information. *IEEE Trans. Instrum. Meas.* **70**, 1–13 (2021).
76. Joyce, C., Burnett, A., Cochrane, J. & Ball, K. Three-dimensional trunk kinematics in golf: between-club differences and relationships to clubhead speed. *Sport. Biomech.* **12**, 108–120 (2013).
77. Severin, A. C., Barnes, S. G., Tackett, S. A., Barnes, C. L. & Mannen, E. M. The required number of trials for biomechanical analysis of a golf swing. *Sport. Biomech.* **00**, 1–9 (2019).
78. Zheng, N., Barrentine, S., Fleisig, G. & Andrews, J. Kinematic analysis of swing in pro and amateur golfers. *Int. J. Sports Med.* **29**, 487–493 (2008).
79. Lai, D. T. H., Hetchl, M., Wei, X., Ball, K. & Mclaughlin, P. On the difference in swing arm kinematics between low handicap golfers and non-golfers using wireless inertial sensors. *Procedia Eng.* **13**, 219–225 (2011).
80. Lindsay, D. M., Mantrop, S. & Vandervoort, A. A. A review of biomechanical differences between golfers of varied skill levels. *Int. J. Sports Sci. Coach.* **3**, 187–197 (2008).
81. Du, S. S. *et al.* How many samples are needed to estimate a convolutional neural network?. *Adv. Neural Inf. Process. Syst.* **2018**, 373–383 (2018).
82. Luo, C. *et al.* How Does the Data set Affect CNN-based Image Classification Performance? In *2018 5th International Conference on Systems and Informatics (ICSAI)* 361–366 (IEEE, 2018). <https://doi.org/10.1109/ICSAI.2018.8599448>.
83. Balki, I. *et al.* Sample-size determination methodologies for machine learning in medical imaging research: A systematic review. *Can. Assoc. Radiol. J.* **70**, 344–353 (2019).
84. Lim, H., Kim, B. & Park, S. Prediction of lower limb kinetics and kinematics during walking by a single IMU on the lower back using machine learning. *Sensors* **20**, 130 (2020).
85. Zihajehzadeh, S., Lee, T. J., Lee, J. K., Hoskinson, R. & Park, E. J. Integration of MEMS inertial and pressure sensors for vertical trajectory determination. *IEEE Trans. Instrum. Meas.* **64**, 804–814 (2015).
86. Hao, M., Chen, K. & Fu, C. Smoother-based 3-D foot trajectory estimation using inertial sensors. *IEEE Trans. Biomed. Eng.* **66**, 3534–3542 (2019).
87. Brown, S. J. *et al.* Determination of the swing technique characteristics and performance outcome relationship in golf driving for low handicap female golfers. *J. Sports Sci.* **29**, 1483–1491 (2011).
88. Glazier, P. S. & Lamb, P. F. Inter- and intra-individual movement variability in the golf swing. In *Routledge International Handbook of Golf Science* Vol. 11 49–63 (Routledge, 2017).
89. Tucker, C. *Is Movement Variability Relevant for the Elite Golfer? A Biomechanical and Modelling Perspective* (2012).

Author contributions

M.K. conceived and designed the study. M.K. carried out the experiments and collected the data. M.K. analyzed the results. S.P. provided supervision and funding for the study. M.K. and S.P. wrote and edited the manuscript. All authors reviewed the manuscript.

Competing interests

The authors declare no competing interests.

Additional information

Correspondence and requests for materials should be addressed to S.P.

Reprints and permissions information is available at www.nature.com/reprints.

Publisher's note Springer Nature remains neutral with regard to jurisdictional claims in published maps and institutional affiliations.



Open Access This article is licensed under a Creative Commons Attribution 4.0 International License, which permits use, sharing, adaptation, distribution and reproduction in any medium or format, as long as you give appropriate credit to the original author(s) and the source, provide a link to the Creative Commons licence, and indicate if changes were made. The images or other third party material in this article are included in the article's Creative Commons licence, unless indicated otherwise in a credit line to the material. If material is not included in the article's Creative Commons licence and your intended use is not permitted by statutory regulation or exceeds the permitted use, you will need to obtain permission directly from the copyright holder. To view a copy of this licence, visit <http://creativecommons.org/licenses/by/4.0/>.

© The Author(s) 2024